Journal of Nuclear Materials xxx (2017) 1–10

Contents lists available at ScienceDirect

Journal of Nuclear Materials

journal homepage: www.elsevier.com/locate/jnucmat

The natural aging of austenitic stainless steels irradiated with fast neutrons

O.V. Rofman [a, b, *], O.P. Maksimkin [a], K.V. Tsay [a], Ye.T. Koyanbayev [c], M.P. Short [d]

[a] Institute of Nuclear Physics, Almaty, Kazakhstan
[b] National University of Science and Technology MISiS, Moscow, Russia
[c] National Nuclear Center, Kurchatov, Kazakhstan
[d] Department of Nuclear Science and Engineering, Massachusetts Institute of Technology, Cambridge, USA

HIGHLIGHTS

- Stress and temperature cause the long timescale evolution of irradiated materials.
- Data challenge the assumption that irradiated materials don't evolve "on the shelf".
- Introduced stress has a significant influence on austenitic steels during storage.
- An important aspect of material aging is the local redistribution of elements.

GRAPHICAL ABSTRACT

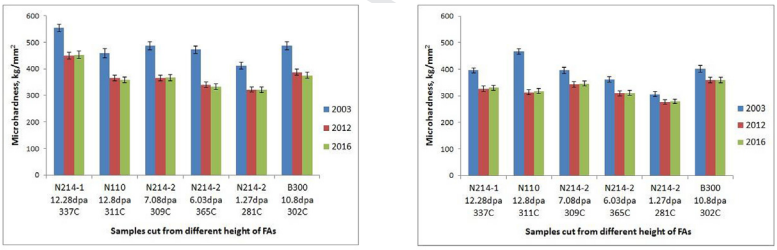

a b

ARTICLE INFO

Article history:
Received 15 June 2017
Received in revised form
10 October 2017
Accepted 5 November 2017
Available online xxx

ABSTRACT

Much of today's research in nuclear materials relies heavily on archived, historical specimens, as neutron irradiation facilities become ever more scarce. These materials are subject to many processes of stress- and irradiation-induced microstructural evolution, including those during and after irradiation. The latter of these, referring to specimens "naturally aged" in ambient laboratory conditions, receives far less attention. The long and slow set of rare defect migration and interaction events during natural aging can significantly change material properties over decadal timescales. This paper presents the results of natural aging carried out over 15 years on austenitic stainless steels from a BN-350 fast breeder reactor, each with its own irradiation, stress state, and natural aging history. Natural aging is shown to significantly reduce hardness in these steels by 10–25% and partially alleviate stress-induced hardening over this timescale, showing that materials evolve back towards equilibrium even at such a low temperature. The results in this study have significant implications to any nuclear materials research program which uses historical specimens from previous irradiations, challenging the commonly held assumptions that materials "on the shelf" do not evolve.

1. Introduction

The reliable integrity of structural nuclear materials, both during service and in subsequent long-term storage, is critical to both nuclear power generation and safe removal of decommissioned radioactive materials. Regular maintenance of nuclear power plants

* Corresponding author. Institute of Nuclear Physics, Almaty, Kazakhstan.
E-mail address: o.rofman@mail.ru (O.V. Rofman).

https://doi.org/10.1016/j.jnucmat.2017.11.006
0022-3115/

requires periodic shuffling and removal of irradiated fuel elements, as well as the continued reliability of structures during operation and decommissioning for further safe storage. All these operations cause structural materials, including fuel assemblies, to incur significant radiation damage in the presence of temperature and stress gradients. Specific operations such as fuel reloading (especially if fuel assembly distortion has taken place), field repairs and welds, and even long-distance transport of irradiated structural materials present major issues to spent fuel integrity in particular, as any unanticipated overloading with respect to the actual mechanical properties of the spent fuel assemblies can result in fuel failure. The additional complication of long-term storage of materials either in spent fuel pools or in laboratories, exacerbated by the current lack of permanent repositories in some countries [1], introduces additional coupled concerns of corrosion to the mix of mechanical property evolution. Knowledge of the specific mechanisms and kinetics leading to deleterious modes of degradation forms the basis of important decisions regarding nuclear materials, ranging from decommissioning procedures [2], to light water reactor (LWR) life extensions [3,4], even to the safety of long-range transport of fuel assemblies in one particularly noteworthy case study from Kazakhstan's BN-350 sodium-cooled reactor [5]. In this case, detailed investigations of mechanical properties were required to conclude that spent fuel assemblies were safe for transport by truck across the country, to protect against accelerations of up to 70 g during postulated transport accidents [6].

Radiation damage ~~itself~~ is arguably one of the most complex multiscale drivers of microstructural evolution [7], with unit atomic processes on the Angstrom-femtosecond scales aggregating through the mesoscale to affect engineering time- and length-scale changes such as fuel cladding creep [8], void swelling [9], and pressure vessel embrittlement [10]. Many major advances have been made in the design and testing of radiation-resistant alloys, a recent, thorough summary of these advances can be found in the work of Odette et al. [11]. However, our continued inability to predict the long-term evolution of radiation-induced microstructural change has resulted in unexpected issues during and after reactor operation, both in thermal and fast reactors. The issue of void swelling for example, long known to the fast reactor community [12] and first predicted to seriously affect LWRs in 1993 [13,14], can take years to decades to occur. Void swelling continues to degrade material properties, especially those under stress, from baffle bolt heads [15] popping off in LWRs [16] to complete embrittlement of fast reactor fuel assembly boxes [17]. Other long-term radiation aging and embrittlement mechanisms, from Cu precipitate formation in LWR pressure vessels [18] to radiation-accelerated spinodal decomposition of stainless steel welds [19] to radiation-induced segregation (RIS) leading to irradiation-assisted stress corrosion cracking (IASCC) [20], all take years or decades to nucleate.

More mysterious, however, is the continued evolution of microstructure even after all major driving forces of elevated temperature, high-flux irradiation, stress, and corrosion due to radiolysis are relieved. This topic has received less attention, despite its increasing potential importance as time goes on. No studies of the continued evolution nor recovery of mechanical properties of irradiated specimens stored "on the shelf" were found. However, analogous studies in austenitic stainless steel welds have shown continued material property and microstructural changes long after their exposure to long-term thermal aging at reactor operating temperatures [21,22]. Case studies were also performed on fuel assemblies stored for 38 years in Obninsk (Russia) [23], and on 321 stainless steel tubing after aging for 17 years [24]. Detailed time-dependent studies have also been performed on the effect of neutron irradiation and long-term aging on mechanical properties and energy characteristics of 0.12C-18Cr-10Ni-Ti austenitic stainless steel [25]. However, less information is available on post-irradiation assessment of aged reactor stainless steels exposed to high doses and long-term monitoring of changes in their properties. Knowledge of the mechanisms and rates of natural aging has the potential to reduce margins for material handling, as even the rare events responsible for evolution back to equilibrium will build up over timescales of decades. Thus quantifying the rate of natural aging actually has the potential to ease aspects of reactor decommissioning and transport, as well as make far more accurate use of popular archival specimen libraries. Based on the results in this study, users of archived sample libraries of irradiated materials, no matter how well documented and characterized, should perform their own confirmatory analyses to ensure good knowledge of the current state of any specimens used.

This study presents mechanical property and electron microscopy data obtained from naturally aged spent fuel assemblies from a BN-350 breeder reactor, under decommissioning since 1999. We show that this natural aging continues to evolve the microstructure of irradiated, stressed materials over decadal timescales, resulting in decreases in irradiation-induced hardening and strengthening. These results imply that irradiated materials recover some of their ductility during natural aging, making them easier to handle in decommissioning, transport, and other activities where they will be subject to external stress which would have induced failure.

2. Experimental procedure

The main materials for investigation were hexagonal fuel assembly shrouds from a number of spent fuel assemblies exposed in a BN-350 breeder reactor in Aktau, Kazakhstan. These fuel assemblies were extracted from both the core and storage pools, where some were aged "wet" in pools and others "dry" in ambient laboratory air. A limited number of fuel assemblies were selected for investigations, these are detailed in Ref. [26]. Other fuel assemblies were packaged in canisters filled with argon and transported to the Semipalatinsk testing site for "dry" storage for about 50 years [6]. The temperature of stored steel elements (cladding of fuel elements and hexagonal shrouds of FAs), according to the calculations [5], can reach 400 °C, though the temperature during natural aging after removal from spent fuel pools was maintained at 20 °C. The operating temperature of the fuel assemblies was relatively low (~300 °C in the bottom end) compared to that for other fast reactors such as EBR-II [27].

Two types of Russian austenitic stainless steels, 0.12C-18Cr-10Ni-Ti (AISI 321 analogue) and 0.08C-16Cr-11Ni-3Mo (AISI 316 analogue) with compositions shown in Table 1, comprised the specimens in this investigation. The shrouds were processed using a final thermo-mechanical treatment consisting of 20% cold drawing followed by temper annealing at 800 °C for 1 h prior to irradiation. All specimens were removed from the flat faces of the shrouds at different distances from the core mid-plane, which represented different irradiation conditions as detailed in Table 2.

Flat specimens for hardness measurements were sliced from the hexagonal shroud of assembly CC-19 at +160 mm and +500 mm perpendicular to the core mid-plane, with dimensions of 13 × 4 × 2 mm. Prior to metallographic studies and microhardness measurements, electropolishing of the austenitic stainless steels was conducted at room temperature using a mixture of 20 ml $HClO_4$ +70 ml C_2H_5OH +70 ml C_3H_8O for 3 s with an applied DC potential of 15 V to remove visible surface oxide layers. The sample sliced from +160 mm was characterized in both a region without noticeable defects and in a noticeably corrosion-affected area with a visible cavity. Vickers microhardness measurements were performed using a PMT-3 hardness gauge with an indenter load of 50 g

Please cite this article in press as: O.V. Rofman, et al., The natural aging of austenitic stainless steels irradiated with fast neutrons, Journal of Nuclear Materials (2017), https://doi.org/10.1016/j.jnucmat.2017.11.006

using a number of reference points on the surface for better statistics. To obtain quantitative changes in microhardness ~~for the studied samples with time~~, the same surface measurements were repeated in 2003, 2012, and 2017 on the same samples, in the same areas between or close to previous Vickers hardness measurements, with the same indentation force, on the same equipment. Electropolishing was required for most samples to remove the oxide layer (3–5 μm) formed on the areas of interest with time. It is worth noting, that additional experiments, performed to check the influence of electropolishing on microhardness, have not shown any significant changes after removal up to 20 μm of material, i.e. this effect is negligible in presented results.

Specimens used for uniaxial tensile tests were sliced from shrouds of N214–1, N214–2, B300 and N110 spent fuel assemblies, with dimensions of 20 × 2.0 × 0.3 mm. Uniaxial tensile testing was initially carried out in 2003 at room temperature with an Instron-1195 tensile testing machine at a strain rate of 8.5×10^{-4} s^{-1}. These specimens were subjected to preliminary grinding and electropolishing to achieve the desired uniform thickness and surface quality. Microhardness measurements were performed immediately after tensile testing using the same Vickers method described above at marked surface reference points along deformed tensile samples. For the following studies, these deformed samples were subject to long-term natural aging while they were stored at room temperature for a few years. Microhardness measurements were repeated on these samples at the same reference points in 2012 and 2017.

A third type of specimen was cut from shrouds of the CC-19 spent fuel assembly at distances of +175 mm, +275 mm, and +315 mm from the core mid-plane, with dimensions of 10 × 3.0 × 0.4 mm. Initial microhardnesses of the specimens were recorded using the methodology described above. The samples were then annealed at 300, 400, and 550 °C for 2600 h and 7000 h in an inert argon atmosphere, and subsequent microhardness measurements were performed.

The effect of natural aging was explored on irradiated materials from two different perspectives: both non-deformed, naturally aged samples and deformed specimens followed by subsequent natural aging. Experiments on high-temperature aging were performed in collaboration between the Institute of Nuclear Physics in Almaty, Kazakhstan and the National Nuclear Center in Kurchatov, Kazakhstan. Magnetic properties of the samples were measured using a Fisher MP-30 Ferroprobe device. Microstructural changes of the third type of samples were studied ~~by means of~~ JEOL JEM-2100 and JEOL 100CX transmission electron microscopes. Disks ~~of~~ 3 mm diameter for TEM studies were prepared from ~300 μm sections. Mechanical grinding and polishing with subsequent electrochemical jet polishing in ~~an electrolyte (~~20 ml $HClO_4$ +70 ml C_2H_5OH +70 ml C_3H_8O~~)~~ were used for final preparation of the TEM specimens.

3. Results

Material property studies of shrouds from the CC-19 fuel assembly associated with phase transformations, swelling, and mechanical characteristics can be found in previous studies [28–31]. The aim of this study was to study the combined effects of neutron irradiation, deformation, and temperature on microstructural changes and, consequently, properties of aged reactor austenitic stainless steels. Microhardness is one of the quantitative indicators that can be used to reflect time-dependent changes taking place in materials of interest, as it is an indicator of the degree of radiation embrittlement due to the formation of numerous types of microstructural defects which impede ductile plastic deformation.

Natural aging aspects for non-deformed exposed samples sliced from the shroud of the CC-19 spent fuel assembly are given in Table 3. Areas affected by corrosion during storage of spent FA (+160 mm) in water pool demonstrated a significant decrease over the first five-year period of dry storage in air. However, it is notable that both specimens taken at +160 mm from the core mid-plane demonstrated almost precisely the same decrease in hardness between 2012 and 2017 (13.4% and 13.5%, respectively), for both the base region and zone of corrosion. The given data shows that strength characteristics of 0.12C-18Cr-10Ni-Ti steel are mainly influenced by both the tendency of material to corrosion, and by the natural aging process itself. The specimen taken from +500 mm from the core mid-plane, subject to half the irradiation dose at 53 °C higher temperature, showed no appreciable decrease in microhardness within margins of error during the same 10 year period of inspection where the +160 mm samples showed 13.5% decreases.

Another approach was to investigate natural aging on materials irradiated with neutrons that were previously deformed, and then stored for a number of years at room temperature. This provided a process more analogous to the natural aging of weld ~~studies~~ [21,22], as the tensile deformation present during weld cooling if not properly relieved represents a similar storage of energy to unannealed irradiation. Mechanical and microstructural characteristics of these materials, irradiated in the BN-350 breeder reactor to different doses, can be found in Refs. [29–33]. Examples of typical microhardness indentations and profiles obtained in 2003 for two irradiated and deformed austenitic steel samples in the form of uniaxial tensile specimens are given in Fig. 1 and Fig. 2, respectively. It was observed that the necking region is characterized by a higher magnetization level compared to that of less deformed areas of tensile specimens. This was attributed to stress-induced $\gamma \rightarrow \alpha$ transformations in the investigated steels [39].

The same ~~points~~ were used as fiducials to repeat microhardness measurements of the studied materials after several more years of natural aging at room temperature. The results shown in Fig. 3 ~~are combined data for aged samples that~~ indicate a trend for a decrease in the microhardness of the deformed, irradiated steels. The idea behind this experiment was that stress, introduced to the material, is accumulated in the form of stored energy. ~~Stored energy~~ could be estimated by amount of defects introduced into the crystallographic lattice. A good example of this estimation for the given steels ~~could~~ be found in Ref. [26]. It is well known that plastic deformation yields measurable amounts of stored energy, which correspond directly to the defects responsible for changing material properties [35,36]. It is likely that natural aging leads to relaxation of accumulated deformation-induced internal stresses in the material that could be illustrated by time-dependent changes in microhardness. This presents a process analogous to the natural aging of irradiation damage shown in the data in Table 3. Notable is

Table 1
Chemical compositions of investigated austenitic steels, wt. %.

Steel Composition	Fe	Cr	Ni	Ti	Mo	C	Si	Mn	P	S
0.12C-18Cr-10Ni-Ti	Bal.	18.24	10.07	0.39	–	0.12	0.34	1.67	0.032	0.013
0.08C-16Cr-11Ni-3Mo	Bal.	16.79	10.49	–	2.47	0.12	0.6	1.46	trace	trace

Please cite this article in press as: O.V. Rofman, et al., The natural aging of austenitic stainless steels irradiated with fast neutrons, Journal of Nuclear Materials (2017), https://doi.org/10.1016/j.jnucmat.2017.11.006

Table 2
Irradiation conditions of austenitic stainless steel samples cut from hexagonal shrouds of spent fuel assemblies exposed in BN-350 breeder reactor.

Fuel assembly	Distance from mid-plane, mm	Steel ~~grade~~	Damage dose, dpa	Dpa rate, $\times 10^{-8}$ dpa/s	Irradiation temp., °C	Experiment description
CC-19	+160	0.12C-18Cr-10Ni-Ti	55.4	113	370	Natural aging (room temperature, 13 years)
	+500	0.12C-18Cr-10Ni-Ti	26.46	54.1	423	
	+175	0.12C-18Cr-10Ni-Ti	55.5	113.2	375	Long-term temperature aging (300 °C, 400 °C,
	+275	0.12C-18Cr-10Ni-Ti	47.3	96.5	400	and 550 °C for 2600 h and 7000 h)
	+315	0.12C-18Cr-10Ni-Ti	45.5	92.8	410	
N214-1	0	0.12C-18Cr-10Ni-Ti	12.28	2.30	337	Tensile testing (room temperature, strain rate
N214-2	−500	0.08C-16Cr-11Ni-3Mo	7.08	2.2	309	8.5×10^{-4} s^{-1}) + natural aging (room temperature, 14 years)
	+500	0.08C-16Cr-11Ni-3Mo	6.03	1.87	365	
	−900	0.08C-16Cr-11Ni-3Mo	1.27	0.39	281	
B300	−500	0.08C-16Cr-11Ni-3Mo	10.8	19.6	302	
N110	0	0.08C-16Cr-11Ni-3Mo	12.8	3.3	311	

Table 3
Timelines of microhardness measurements of naturally aged specimens of 0.12C-18Cr-10Ni-Ti steel irradiated to 55.4 dpa and 26.46 dpa in the BN-350 breeder reactor.

Distance from core mid-plane, mm	Specimen description	Usage period	Placed in pool	Year of study/Microhardness[a], kg/mm^2				
				Nov., 2004	Dec. 2009	Jan., 2007	Mar., 2012	Feb., 2017
+160	Base region	March 1979–May 1981	May 1981	380	382	–	388	336
	Corrosion zone			244	199	–	200	173
+500	Base region			–	–	312	–	306

[a] Measurements error did not exceed 3%.

the fact that high-dose irradiation to the point of total material embrittlement in the studies in Table 3 and uniaxial stress testing to failure in the studies in Fig. 3 produce decreases in microhardness of the same magnitude, about 15% in most cases in the necking region where failure occurred. This corresponds to a prediction by Averback et al., which stated that there is a maximum possible defect concentration universal to all materials [37], which would result in a related maximum energy storage capability of materials regardless of the deformation or damage mode.

Long-term thermal aging experiments, performed between 300 and 550 °C on 0.12C-18Cr-10Ni-Ti steel irradiated with neutrons, illustrate a certain decrease in strength characteristics of aged materials. Aging for 2600 h and 7000 h, as expected, resulted in a decrease of microhardness at temperatures of 400 °C and higher compared to initial values (Fig. 4). Lower annealing temperatures showed a slight increase in steel hardness ~~that~~ was attributed to both carbide formation and material heterogeneity. The mean grain size of the annealed material for 2600 h showed an insignificant increase from 12 μm (300 °C) to 15 μm (550 °C). A similar grain growth rate was observed for the samples annealed for 7000 h that characterizes the stability of grain microstructure in this steel at the given temperatures.

TEM images of irradiated 0.12C-18Cr-10Ni-Ti steel followed by aging at 550 °C for 2600 h (Fig. 5) reflect the most notable microstructural characteristics of the material. The mean void size was observed to be ~30 nm with a void volume fraction of ~10%. The observed dislocation density is relatively low, which is more typical of thermally aged materials. Large (~130 nm) and fine (up to 30 nm) spherical inclusions were observed to be randomly distributed in the matrix (Fig. 5a–b). Both morphologies were mainly comprised of primary and secondary Ti carbides. Spherical or elliptical particles were also located at grain boundaries (Fig. 5c). The irradiated steel was characterized by the presence of denuded zones at grain boundaries (Fig. 5c–d).

A characteristic feature of the observed inclusions is the complex morphology that often gives the mistaken impression of a single particle. One of the examples is the segregation of primary TiC surrounded by a shield of secondary $Cr_{23}C_6$ (Fig. 5c), observed at grain boundaries and in the matrix.

The complex morphology of inclusions was additionally confirmed by EDS mapping of element distributions at grain boundaries of the 0.12C-18Cr-10Ni-Ti steel irradiated with neutrons (Fig. 6). The ~~obtained~~ data indicate that an accumulation of alloying elements is observed at the grain boundaries, and large inclusions are characterized by an increased Ti concentration in the central part of the inclusion, while the periphery is surrounded by Cr and Ni. A small accumulation of charge on the specimen did not allow for quantitative mapping due to drifting and scanning time, but did illustrate the overall picture.

A quantitative estimate of the distribution of elements in irradiated and aged 0.12C-18Cr-10Ni-Ti steel is presented in Fig. 7. The microstructure is characterized by some depletion of chromium at the grain boundary (with simultaneous segregation around the inclusions), in comparison with concentration in the grain matrix. Theoretically, this creates a certain threat associated with the potential risk of developing intergranular corrosion under conditions of interaction with the coolant and with further improper storage in the soaking basin. More detailed data on the redistribution of elements in the border areas of irradiated austenitic stainless steels are given in Ref. [13].

G-phase precipitation, crystallographically identified as having an FCC structure (space group Fm3m, lattice parameter 1.09 nm, 1.12 nm and 1.14 nm), was also identified in the irradiated and aged microstructure. The observed G-phase is considered to be an intermetallic silicide (Ni-Si-Ti) with many variations in stoichiometry reported [40]. Fig. 8 shows bright and dark field TEM images that illustrate G-phase (diffraction pattern includes intensive reflexes of the matrix and weak reflexes of G-phase located close to the central beam). EDS analysis performed at the area containing G-phase particles shows a slight increase in Si and Ni concentrations

Please cite this article in press as: O.V. Rofman, et al., The natural aging of austenitic stainless steels irradiated with fast neutrons, Journal of Nuclear Materials (2017), https://doi.org/10.1016/j.jnucmat.2017.11.006

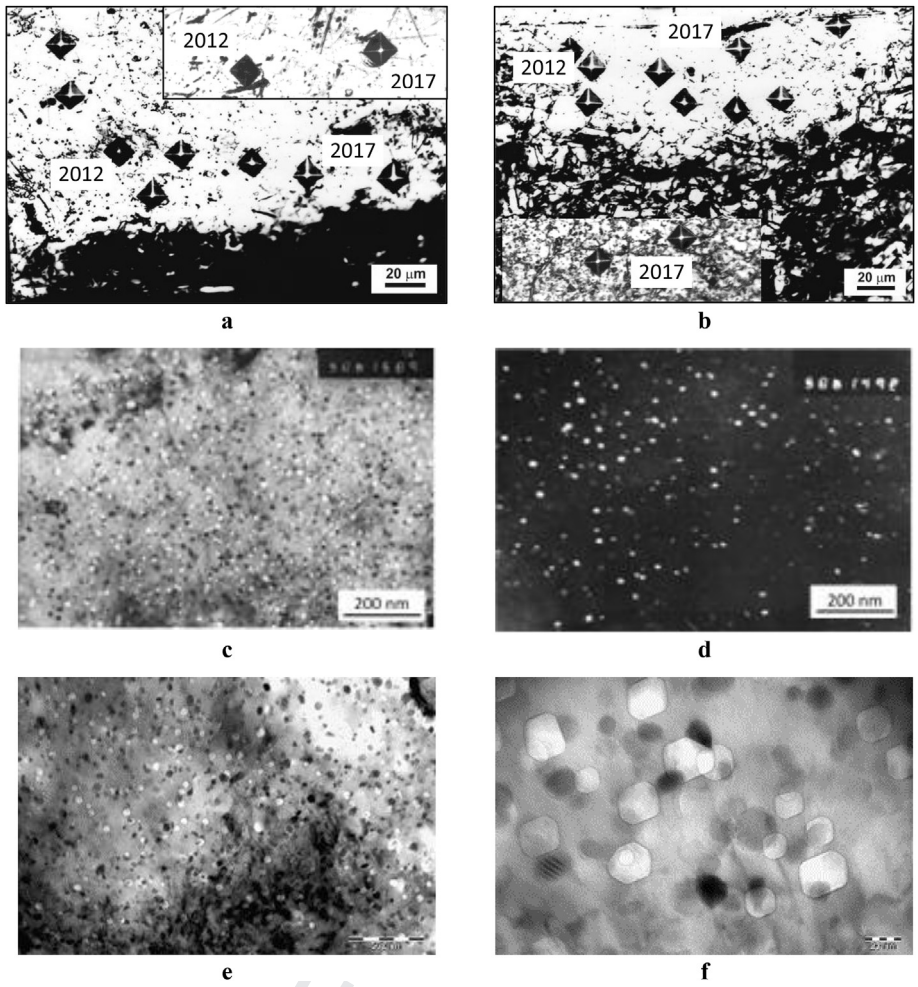

Fig. 1. Representative microhardness indentations on 0.12C-18Cr-10Ni-Ti steel (CC-19, +160 mm) measured in 2012 and 2017 for regions (a) unaffected and (b) affected by corrosion; (c–d) BF and DF TEM images taken from the CC-19 ("+160 mm") sample in 2004; (e–f) TEM images taken from the same CC-19 ("+160 mm") sample in 2017.

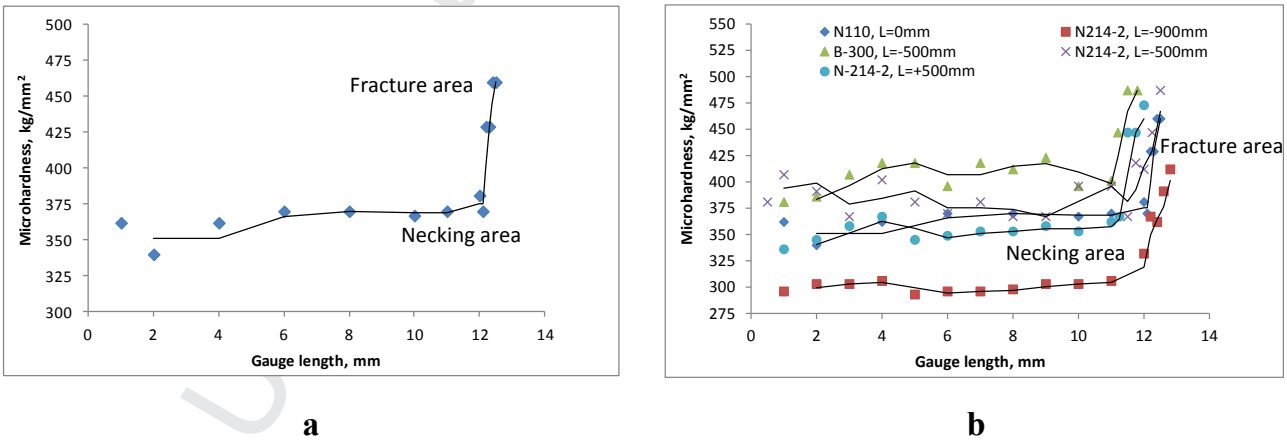

Fig. 2. Michrohardness distribution (measurements performed in 2003) along the gauge length of the irradiated stainless steels deformed to failure (a) 0.12C-18Cr-10Ni-Ti, (N214-1 FA, «0 mm», 12.28 dpa, T = 337 °C) and (b) 0.08C-16Cr-11Ni-3Mo (N110, B300 and N214-2 FAs).

(Table 4).

4. Discussion

When discussing the obtained results, it is necessary to focus on the following factors that, to some extent, influence the aging of the material. First, the effect of room temperature (natural aging) on the properties of the studied irradiated austenitic stainless steels is relatively low at short times, while extended natural aging does produce significant decreases in microhardness regardless of

Please cite this article in press as: O.V. Rofman, et al., The natural aging of austenitic stainless steels irradiated with fast neutrons, Journal of Nuclear Materials (2017), https://doi.org/10.1016/j.jnucmat.2017.11.006

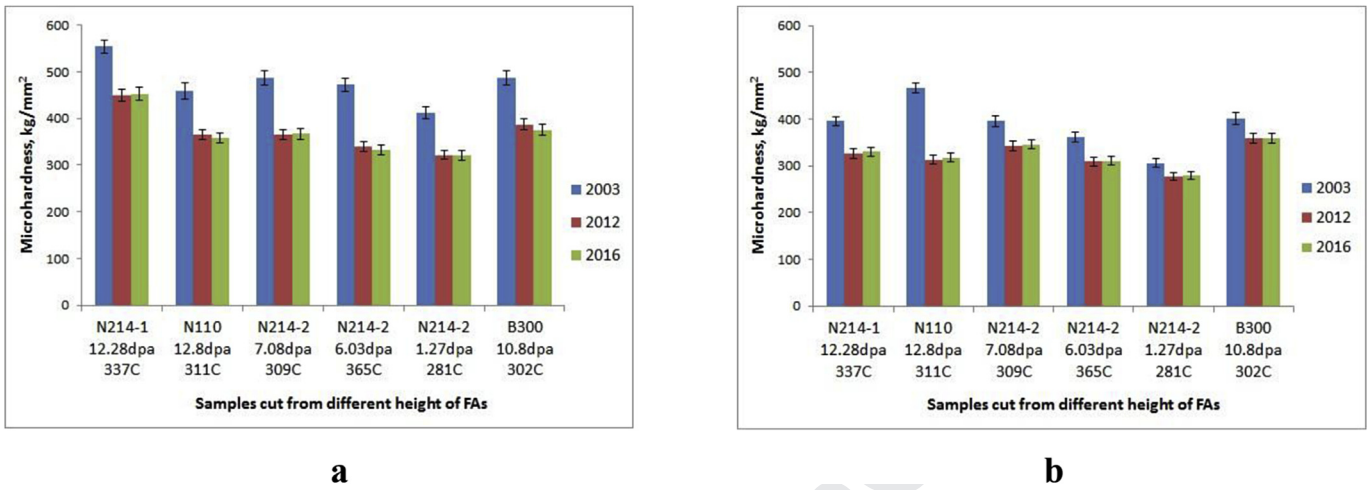

Fig. 3. Microhardness changes due to natural aging (2003–2016) at room temperature in 0.12C-18Cr-10Ni-Ti (N241-1 FA) and 0.08C-16Cr-11Ni-3Mo (N214–2, N110 and B300 FAs) steels irradiated with neutrons at different temperatures to various damage doses (a) in the fracture area and (b) in the necking area of uniaxial tensile specimens.

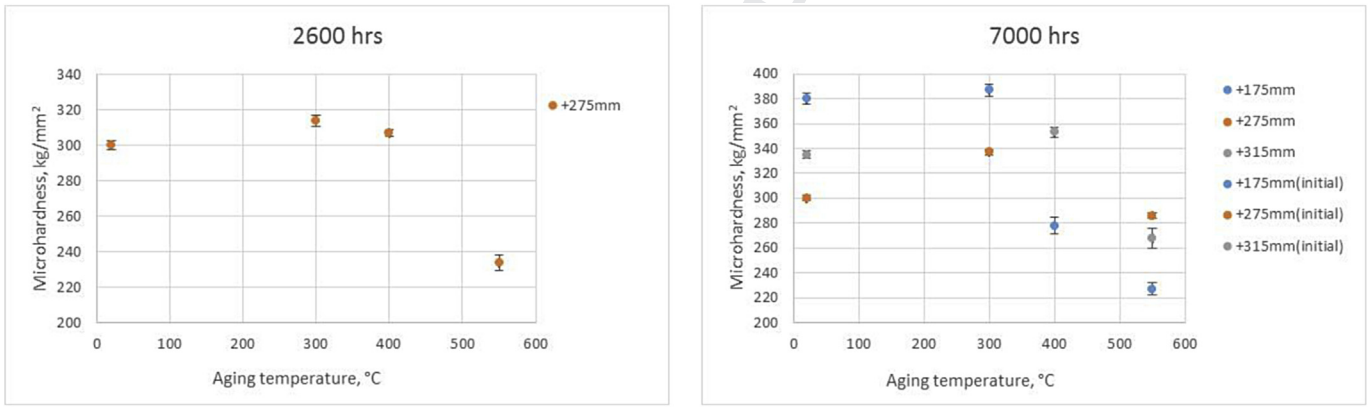

Fig. 4. Microhardness changes resulting from thermal aging of 0.12C-18Cr-10Ni-Ti steel for (a) 2600 h and (b) 7000 h of the neutron irradiated samples sliced from the shroud of the CC-19 spent fuel assembly at different distances from the core mid-plane.

location in the corroded or uncorroded zone of fuel shrouds. The determining factors that influence given design characteristics of steels are the storage conditions of spent materials in the water pools (control of water purity, observance of ~~the~~ temperature ~~regime~~ and the stress~~ed~~ state of the structural units). In fact, the low chlorine concentration was specifically cited as a reason these particular BN-350 assemblies experienced so little corrosion [38]. Secondly, stress initially introduced by irradiation and followed by subsequent deformation has a long term impact on the material. The higher the damage dose, the more serious destabilization it causes to the stress state of the material, as evidenced by microhardness and magnetic measurements in the fracture zone. Examples where this is expected to be important include irradiation-induced swelling, creep, thermal gradients, and phase transformations.

It can be asserted that the decrease in microhardness is associated with microstructural changes occurring in the material with time. Changes taking place during long-term aging will affect point defects and impurity atoms frozen in the microstructure, and also affect the quantitative characteristics of large defects – loops, pores, second phase particles. Fig. 1(c–f) illustrates the microstructures obtained from the same sample in 2004 and 2017. It is difficult to observe changes that lead to an increase in microhardness by 10–15%, but some changes in the porous structure and in the size of the secondary phase are observed. As can be seen from the illustrations, the number of defects decreases, and their dimensions increase somewhat. One can ~~note~~ a noticeable increase in the ~~particles of the secondary phases.~~ The removal of point defects and impurity atoms on ~~the~~ sinks, in particular, grain boundaries, the surface of secondary precipitates, pores, etc., leads to the enlargement of a number of defects and the softening of the matrix. At the same time, due to the recombination processes ~~going on~~, some of the small defects can disappear. More significant changes in the microstructure were illustrated in a previous study [41] on steel samples studied after irradiation in the WWR-K reactor and subjected to post-radiation annealing in the temperature range 450–1050 °C.

The observed decrease in the strength characteristics of irradiated austenitic steels can be attributed to a number of factors, many of which have been documented in the literature. One is certainly due to internal stress relaxation that happens with time, both from reduction in the number of radiation defects present and due to the reversal of radiation-induced martensitic phase transformation. The strongest effect of reducing the strength characteristics is

Please cite this article in press as: O.V. Rofman, et al., The natural aging of austenitic stainless steels irradiated with fast neutrons, Journal of Nuclear Materials (2017), https://doi.org/10.1016/j.jnucmat.2017.11.006

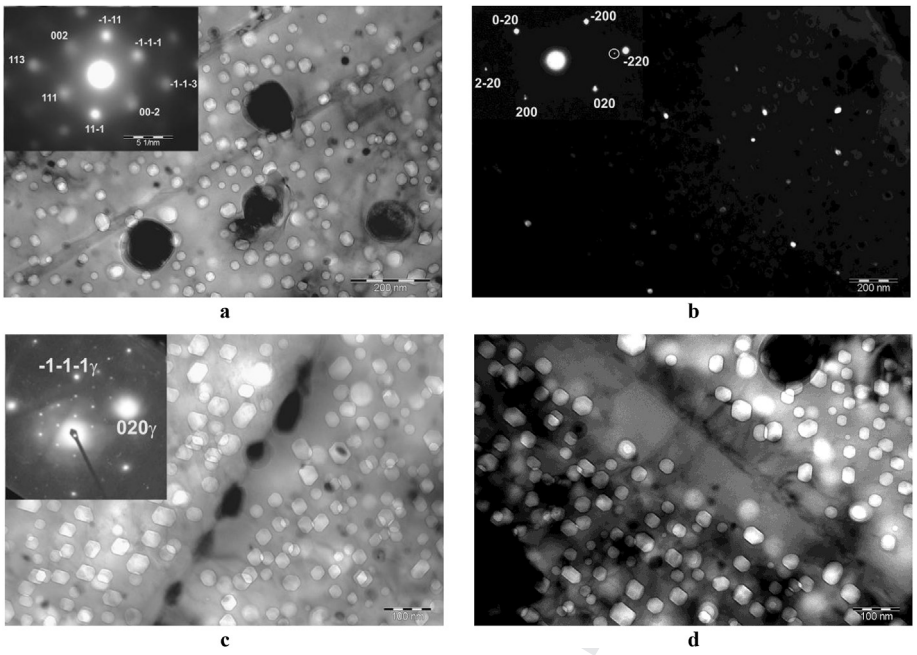

Fig. 5. TEM images and diffraction patterns of irradiated 0.12C-18Cr-10Ni-Ti steel (47.3 dpa, 400 °C) after aging at 550 °C for 2600 h in argon: (a) primary TiC carbides, [1$\bar{1}$0] zone axis; (b) dark field image of secondary TiC carbides, [001] zone axis; (c) $M_{23}C_6$ inclusions at a grain boundary, [001] zone axis; (d) denuded zones at a grain boundary.

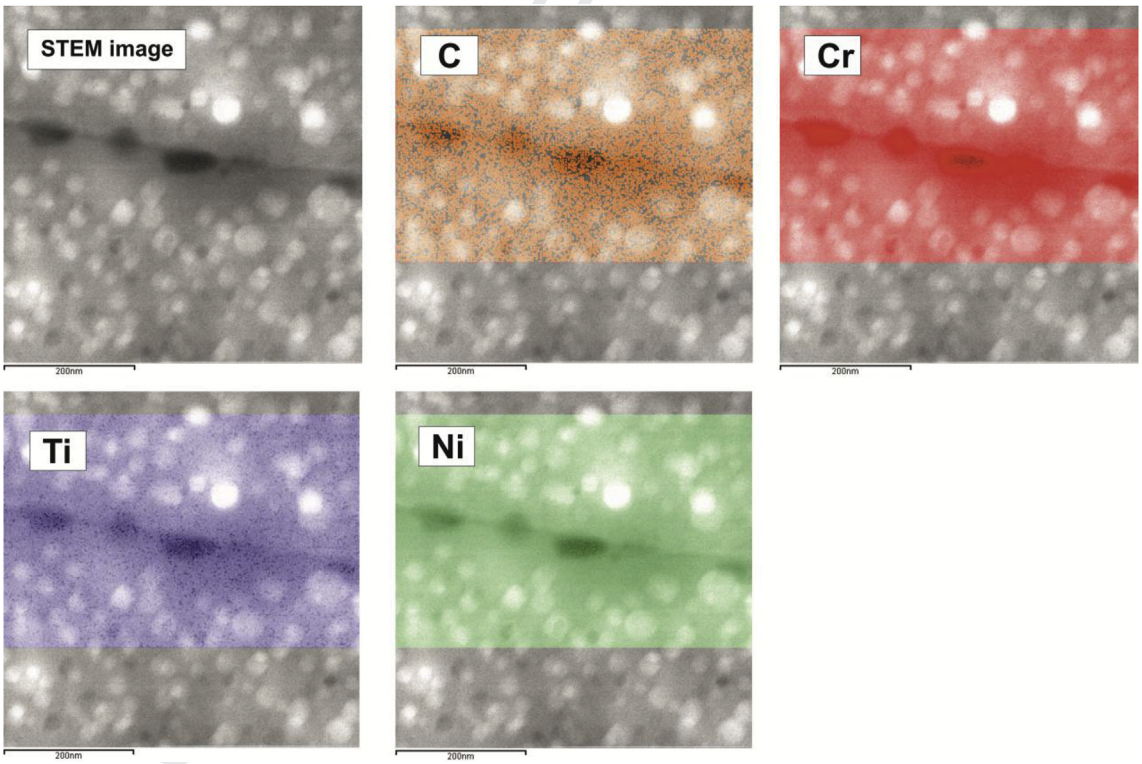

Fig. 6. STEM image and corresponding near-grain boundary EDX mapping for 0.12C-18Cr-10Ni-Ti steel after aging at 550 °C for 2600 h in argon.

manifested at dry storage stages in areas subject to intergranular corrosion. It should, however, be noted that aggressive reagents used for electropolishing the samples may play a role, and may also remain on the samples in small quantities. The third aspect, which requires attention during operation and post-operational storage of steels, is the phase transformations and redistribution of alloying elements. Phase transformations, such as $\gamma \rightarrow \alpha'$ and reversed $\alpha' \rightarrow \gamma$ martensitic transformations [34], are some of the accommodation mechanisms resulting from external factors (irradiation-induced stress, temperature) that affect both microstructural characteristics and mechanical properties of the materials. The effect of redistribution of ~~composition~~ elements in the austenitic steels causes a

Please cite this article in press as: O.V. Rofman, et al., The natural aging of austenitic stainless steels irradiated with fast neutrons, Journal of Nuclear Materials (2017), https://doi.org/10.1016/j.jnucmat.2017.11.006

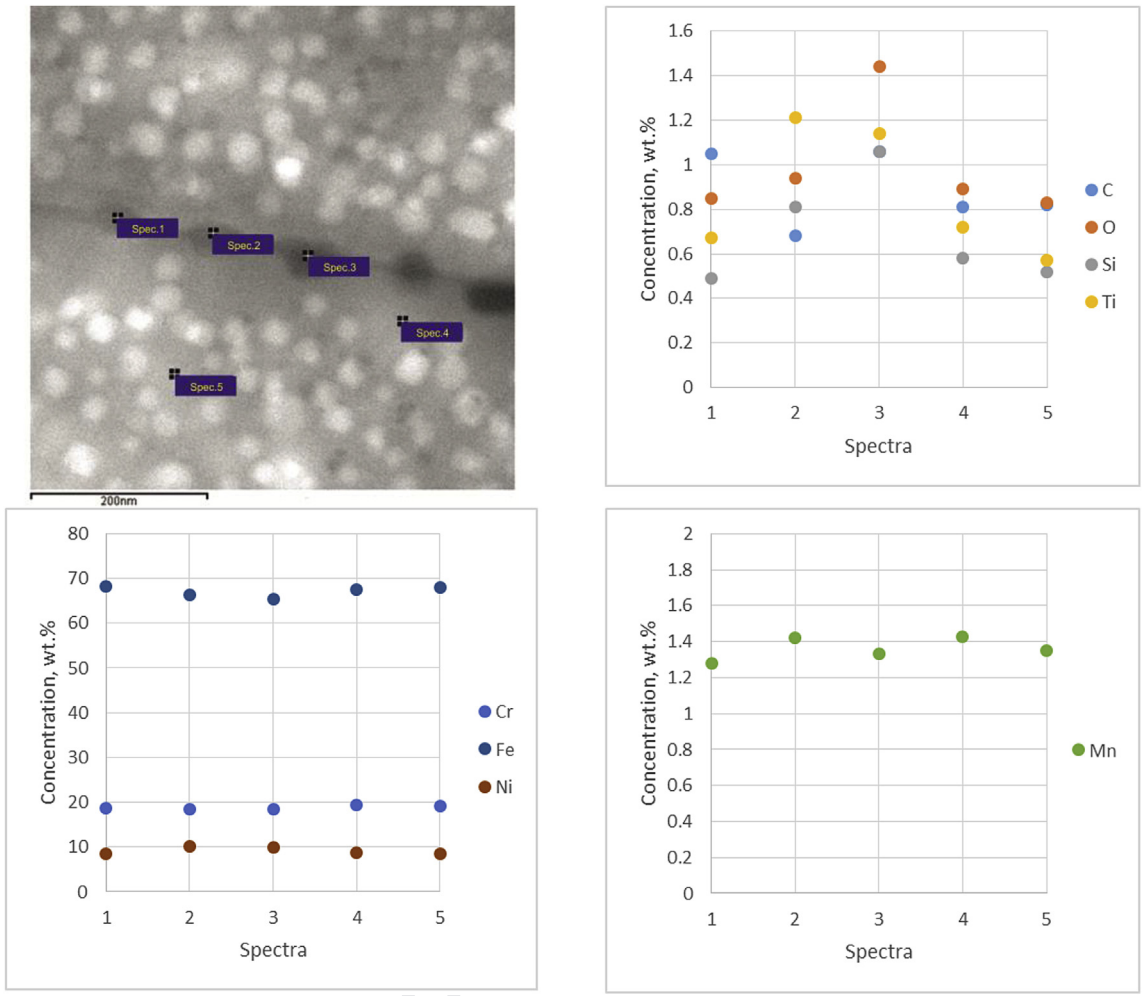

Fig. 7. Element concentrations at a near-grain boundary area of the 0.12C-18Cr-10Ni-Ti steel after aging the sample at 550 °C for 2600 h in argon as measured by point EDX spectra.

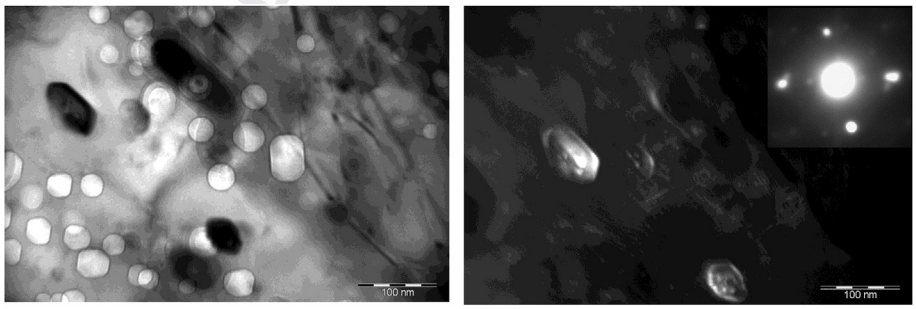

a b

Fig. 8. Second-phase particles in ~~the~~ irradiated 0.12C-18Cr-10Ni-Ti steel (47.3 dpa, 400 °C) after aging at 550 °C for 2600 h in argon: (a) bright field and (b) dark field TEM images of precipitates.

potential danger to maintain resistance to corrosion during wet storage. Interestingly, the process of natural aging may actually decrease the propensity for accelerated corrosion or cracking to occur should aged fuel assemblies be moved at a much later date, as studies have shown that cracking and irradiation-induced stress corrosion cracking (IASCC) is exacerbated by hardening, radiation induced segregation (RIS), and other effects [42]. Many of these are shown to self-ameliorate, albeit slowly, during natural aging.

The largest likely contributor to the observed reduction in hardness is the slow, but steady emission of point defects from small radiation damage clusters, coupled together with their more rapid diffusion enabled by ~~the~~ radiation-induced changes in the microstructure. Fig. 1c–d shows how a plethora of small precipitates and secondary phases have formed as a result of irradiation, while Fig. 1e–f shows considerable coarsening over time. This coarsening is reminiscent of cluster dynamics models, which

Please cite this article in press as: O.V. Rofman, et al., The natural aging of austenitic stainless steels irradiated with fast neutrons, Journal of Nuclear Materials (2017), https://doi.org/10.1016/j.jnucmat.2017.11.006

Table 4
G-phase composition in 0.12C-18Cr-10Ni-Ti steel irradiated to 47.3 dpa at 400 °C after aging at 550 °C for 2600 h.

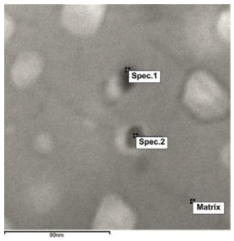

Elements/Spectrum	Element composition, wt. %						
	Si	Ti	Cr	Mn	Fe	Ni	Total
Precipitate 1	0.88	0.96	19.38	1.35	67.92	9.50	100.00
Precipitate 2	0.86	0.88	19.50	1.35	68.23	9.19	100.00
Matrix	0.78	0.85	19.51	1.34	68.44	9.08	100.00

generally show an increase in mean defect size and a reduction in number of clusters over time [43]. Similar microstructures with extremely high internal interface areas have been shown to greatly increase diffusion by increasing diffusion prefactors (available sites for rapid diffusion), for the case of Cr in nanocrystalline Fe [44].

It has been recently shown that such very small defect clusters comprise the majority of radiation damage [45,46], and that they are primarily responsible for substantial changes in mechanical properties [47]. Therefore, the increased fast diffusion paths created by the evidently high number of coherent and incoherent precipitates (as well as the dislocation forest that is not TEM-visible), combined with the propensity for the more numerous, smaller clusters to emit rather than absorb point defects, is simultaneously responsible for the coarsening of visible defects and for the reduction in microhardness ~~observed~~.

Most important is the finding that materials subject to any significant energy storage, be it by irradiation, stress, or both, *do* measurably relax towards an equilibrium, less stressed state at room temperature in ambient conditions. This challenges a potential assumption that materials kept in controlled laboratory conditions are kept at static equilibrium, essentially "frozen in place" until subsequent investigations are made. Instead the results in this study, particularly those in Fig. 3 and Table 3, motivate a closer look at any specimen that has sat on the shelf for periods of years to decades. Plenty of studies have focused on the effects of thermal aging separate from irradiation effects [48–50] which typically follow Arrhenius rate laws, though ours shows that archival specimens do indeed age as one would expect over exceedingly long timescales at very low temperatures compared to prior studies. As an example, we propose the following way to calculate activation energy from the data obtained for 0.12C-18Cr-10Ni-Ti steel (CC-19 FA, "+275 mm") after high-temperature aging for 2600 and 7000 h. First step is to modify the original Arrhenius equation ($k = Ae^{-Q/RT}$) by substituting the rate constants (k) for $\frac{H_m}{t}$ (H_m – microhardness, kg/mm^2; t – annealing time). This, in our opinion, reflects the rate at which changes take place in the steel over time and gives: $\frac{H_m}{t} = Ae^{-Q/RT}$. The pseudo-activation energy Q ~~then can~~ be calculated by combining the two equations:

$$Q = \frac{RT_1T_2}{(T_1-T_2)}\ln\left(\frac{\frac{H_{m1}}{t_1}}{\frac{H_{m2}}{t_2}}\right) = \frac{8.314*573*823}{(573-823)}\ln\left(\frac{\frac{337}{7200}}{\frac{234}{2600}}\right) = 10253 \text{ J/mol.}$$

These types of archival specimens comprise a significant portion of prior and current work in nuclear structural materials, as much extra material exists from previous irradiation campaigns and neutron sources continue to become more scarce. The authors therefore recommend more careful determination of any natural aging in archived, irradiated specimens via a convenient method, such as microhardness measurement, before drawing any quantitative or mechanistic conclusions about the material properties or defect/microstructural evolution observed in archival specimens.

5. Conclusions

The aging of irradiated austenitic steels has been studied from the standpoint of long wet and dry storage of materials, prolonged thermal impact, and introduced stress. In particular, the effect of "natural aging" at ambient laboratory conditions was shown to have an effect on both irradiated and stressed austenitic stainless steels. Microhardness was used as a quantitative criterion to estimate changes in the mechanical characteristics of materials over time. The obtained data made it possible to conclude that the introduced stress (during operation or after strength tests) has a significant influence on the subsequent behavior of austenitic steels during storage. Natural aging is characterized by a tendency to decrease the microhardness of austenitic steels due to a decrease in the energy accumulated by the material in the form of defects introduced into the crystal lattice. ~~Thermal contribution~~ during accelerated aging tests ~~has a significant effect~~ at temperatures above 400 °C, when the irradiated material (especially exposed to large damage doses) begins to lose its strength characteristics. A lower temperature promotes the formation of carbide-forming compounds, which contribute to hardening of the material. An important aspect in the process of material aging is the local redistribution of elements in the matrix and along the grain boundaries. The data challenge the commonly held assumption that irradiated materials do not evolve "on the shelf," prompting a more careful look at any archival specimens years to decades old.

Uncited references

[34]; [42].

Acknowledgements

The authors would like to thank researchers that worked at the Laboratory of Radiation Materials Science at the Institute of Nuclear Physics (INP) over the years for their contributions to this publication. M.P.S. acknowledges financial support from the MIT's MISTI Global Seed Fund (GSF) for enabling this collaboration, and from the U.S. Nuclear Regulatory Commission's MIT Nuclear Education Faculty Development Program under Grant No. NRC-HQ-84-15-G-0045. O.V.R. gratefully acknowledges the financial support of the Ministry of Education and Science of the Russian Federation in the framework of Increase Competitiveness Program of NUST « MISiS» (№ К4-2017-058), implemented by a governmental decree dated 16th of March 2013, N 211.

References

[1] R.P. Rechard, H.-H. Liu, Y.W. Tsang, S. Finsterle, Site characterization of the Yucca Mountain disposal system for spent nuclear fuel and high-level radioactive waste, Reliab. Eng. Syst. Saf. 122 (2014) 32.
[2] J. Bohmert, K. Torronen, M. Valo, Reexamination of reactor pressure-vessels of

the decommissioned greifswald nuclear-power-plant - opportunity for realistic evaluation of neutron embrittlement, in: Annual Meeting on Nuclear Technology '96, Rosengarten, Germany, May 21-23, 1996, pp. 176–179.
[3] E.A. Kenik, J.T. Busby, Radiation-induced degradation of stainless steel light water reactor internals, Mater. Sci. Eng. Rep. 73 (7–8) (2012) 67.
[4] M. Kolluri, A. Kryukov, A.J. Magielsen, et al., Mechanical properties and microstructure of long term thermal aged WWER 440 RPV steel, J. Nucl. Mater. 486 (2017) 138.
[5] D.N. Olsen, J.D.B. Lambert, H.P. Planchon, E.A. Howden, S.V. Krechetov, V.N. Karaulov, S.M. Koltyshev, J. Gerrard, Development of the safety case for a spent fuel dry storage facility in Kazakhstan, a case study, in: International Conference on Nuclear Engineering (ICONE); Nice, Acropolis (France); 8–12 Apr, 2001. http://www.iaea.org/inis/collection/NCLCollectionStore/_Public/33/020/33020132.pdf. (Accessed 26 May 2017).
[6] J.D.B. Lambert, et al., Characterizing and packaging BN-350 spent fuel for long-term dry storage, in: International Workshop "Nuclear Power Technologies", 2000, pp. 86–87. Accessed at, https://inis.iaea.org/search/search.aspx?orig_q=RN:31065467. (Accessed 27 May 2017).
[7] M.P. Short, S. Yip, Materials aging at the mesoscale: kinetics of thermal, stress, radiation activations, COSSMS 19 (4) (2015) 245–252.
[8] R.A. Holt, In-reactor deformation of cold-worked Zr-2.5Nb pressure tubes, J. Nucl. Mater. 372 (2–3) (2007) 182.
[9] F.A. Garner, M.B. Toloczko, Irradiation creep and void swelling of austenitic stainless steels at low displacement rates in light water energy systems, J. Nucl. Mater. 251 (1997) 252.
[10] M.K. Miller, K.F. Russell, Embrittlement of RPV steels: an atom probe tomography perspective, J. Nucl. Mater. 371 (1–3) (2007) 145.
[11] G.R. Odette, M.J. Alinger, B.D. Wirth, Recent developments in irradiation-resistant steels, Ann. Rev. Mater. Sci. 38 (2008) 471.
[12] E.A. Little, D.A. Stow, Void-swelling in irons and ferritic steels, 2. Experimental survey of materials irradiated in a fast-reactor, J. Nucl. Mater. 87 (1) (1979) 25.
[13] F.A. Garner, L.R. Greenwood, D.L. Harrod, Potential high fluence response of pressure vessel internals constructed from austenitic stainless steels, in: Proc. Sixth Intl. Symp. Env. Deg. Mater. Nucl. Power Systems - Water Reactors, San Diego, CA, 1993, pp. 783–790.
[14] F.A. Garner, M.B. Toloczko, Irradiation creep and void swelling of austenitic stainless steels at low displacement rates in light water energy systems, J. Nucl. Mater. 251 (1997) 252–261.
[15] D.J. Edwards, E.P. Simonen, F.A. Garner, et al., Influence of irradiation temperature and dose gradients on the microstructural evolution in neutron-irradiated 316SS, J. Nucl. Mater. 317 (1) (2003) 32.
[16] F.M. Gregory, S. Fyfitch, Baffle bolt failures - a B&W owners group approach, Nucl. Eng. Des. 192 (2–3) (1999) 345.
[17] V.S. Neustroyev, Z.Y. Ostrovskiy, V.K. Shamardin, Influence of stresses on radiational swelling and vacancy porosity parameters of neutron irradiated austenite steels, Fiz. Met. I Metalloved. 86 (1) (1998) 115.
[18] G.R. Odette, G.E. Lucas, Recent progress in understanding reactor pressure vessel steel embrittlement, Rad. Eff. Defects Solids 144 (1–4) (1998) 189.
[19] T. Takeuchi, Y. Kakubo, Y. Matsukawa, et al., Effects of neutron irradiation on microstructures and hardness of stainless steel weld-overlay cladding of nuclear reactor pressure vessels, J. Nucl. Mater. 449 (1–3) (2014) 273.
[20] J.T. Busby, G.S. Was, E.A. Kenik, Isolating the effect of radiation-induced segregation in irradiation-assisted stress corrosion cracking of austenitic stainless steels, J. Nucl. Mater. 302 (1) (2002) 20.
[21] K. Chandra, V. Kain, V. Bhutani, V.S. Raja, R. Tewari, G.K. Dey, J.K. Chakravartty, Low temperature thermal aging of austenitic stainless steel welds: kinetics and effects on mechanical properties, Mater. Sci. Eng. A 534 (2012) 163.
[22] S.H. Hong, M.-G. Seo, C.H. Jang, K.-S. Lee, Evaluation of the effects of thermal aging of austenitic stainless steel welds using small punch test, Procedia Eng. 130 (2015) 1010.
[23] S.N. Ivanov, Yu.V. Konobeev, O.V. Starkov, S.I. Porollo, A.M. Dvoryashin, S.V. Shulepin, Materials-technology investigations of fuel elements, irradiated in a reactor at the Obninsk nuclear power plant, after standing for 38 years in a depository, At. Energy 88 (3) (2000) 184.
[24] J.M. Leitnaker, J. Bentley, Precipitate phases in type 321 stainless steel after aging 17 years at ~600°C, Metall. Trans. A 8 (1977) 1605.
[25] M.N. Gusev, O.P. Maksimkin, The effect of neutron irradiation and long-term storage on mechanical and energy characteristics of stainless steel, Phys. Met. Metallogr. 92 (5) (2001) 77.
[26] V.N. Karaulov, et al., BN-350 reactor fuel condition after irradiation and storage in cooling pool, Vestn. Natsional'nogo Yad. Tsentra Resp. Kazakhstan 1 (5) (2001) 59. https://inis.iaea.org/search/search.aspx?orig_q=RN:35045569.
[27] J.E. Cahalan, T.A. Taiwo, Liquid Salt – Very High Temperature Reactor: Survey of Sodium-cooled Fast Reactor Fuel Handling Systems for Relevant Design and Operating Characteristics, 2006, p. 3. Tech. Report No. ANL-GenIV-069.
[28] O.P. Maksimkin, K.V. Tsay, F.A. Garner, Inhomogeneity of microstructure, mechanical properties, magnetism, and corrosion observed in a 12Cr18Ni10Ti fuel assembly shroud irradiated in BN-350 to 59 dpa, J. Nucl. Mater. 467 (2015) 899.
[29] M.N. Gusev, O.P. Maksimkin, F.A. Garner, Peculiarities of plastic flow involving "deformation waves" observed during low-temperature tensile tests of highly irradiated 12Cr18Ni10Ti and 08Cr16Ni11Mo3 steels, J. Nucl. Mater. 403 (2010) 121.
[30] O.P. Maksimkin, K.V. Tsai, L.G. Turubarova, T. Doronina, F.A. Garner, Void swelling of AISI 321 analog stainless steel irradiated at low dpa rates in the BN-350 reactor, J. Nucl. Mater. 367–370 (2007) 990.
[31] M.N. Gusev, O.P. Maksimkin, O.V. Tivanova, N.S. Silnaygina, F.A. Garner, Correlation of yield stress and microhardness in 08Cr16Ni11Mo3 stainless steel irradiated to high dose in the BN-350 fast reactor, J. Nucl. Mater. 359 (2006) 258.
[32] O.V. Rofman, K.V. Tsay, O.P. Maksimkin, The defect microstructure and element composition in denuded zones of stainless steels irradiated in BN-350 nuclear reactor, MRS Adv. Vol. 2, Issue 21-22 (Energy and Sustainability), (2017), 1209-1215.
[33] K.K. Kadyrzhanov, S.B. Kislitsin, O.P. Maksimkin, O.G. Romanenko, T.E. Turkebaev, Degradation in mechanical properties of stainless steels C0.12Cr18Ni10Ti and C0.08Cr16Ni11Mo3 – materials for hexagonal ducts of spent fuel assemblies from the BN-350 fast neutron reactor, in: Safety Related Issues of Spent Nuclear Fuel Storage: Strategies for Safe Storage of Spent Fuel, Springer, 2007, pp. 329–349.
[34] O.P. Maksimkin, Deformation induced martensitic transformation in Cr–Ni stainless steel irradiated by neutrons, Phys. Stat. Sol. A 163 (1997) R7.
[35] M. Verdier, I. Groma, L. Flandin, et al., Dislocation densities and stored energy after cold rolling of Al-Mg alloys: investigations by resistivity and differential scanning calorimetry, Scr. Mater. 37 (4) (1997) 449.
[36] T. Knudsen, W.Q. Cao, A. Godfrey, et al., Stored energy in nickel cold rolled to large strains, measured by calorimetry and evaluated from the microstructure, Metal. Mater. Trans. A 39A (2) (2008) 430.
[37] R.S. Averback, K.L. Merkle, Radiation annealing effects in energetic displacement cascades, Phys. Rev. B 16 (1977) 3860.
[38] V.N. Karaulov, A.P. Blynski, S.V. Golovnin, I.K. Yakovlev, E.V. Chumakov, K.K. Kadyrzhanov, H.G. Kadyrov, T.E. Turkebaev, J.D.B. Lambert. BN-350 core and blanket fuel condition after irradiation and wet storage. International Work-shop "Nuclear Power Technologies" (NPT-2000), IAEA Tech. Report No. INIS-KZ–068, Accessed at http://www.iaea.org/inis/collection/NCLCollectionStore/_Public/31/065/31065450.pdf on 2017-05-27.
[39] K.K. Kadyrzhanov, O.P. Maksimkin, Martensitic transformations in neutron irradiated and helium implanted stainless steels, in: M.L. Grossbeck, et al. (Eds.), Effects of Radiation on Materials: 21st International Symposium, ASTM International, 2004, pp. 105–123.
[40] I. Shuro, H.H. Kuo, T. Sasaki, K. Hono, Y. Todaka, M. Umemoto, G-phase precipitation in austenitic stainless steel deformed by high pressure torsion, Mater. Sci. Eng. A 552 (2012) 194.
[41] K.V. Tsay, O.P. Maksimkin, L.G. Turubarova, O.V. Rofman, F.A. Garner, Microstructural defect evolution in neutron-irradiated 12Cr18Ni9Ti stainless steel during subsequent isochronous annealing, J. Nucl. Mater. 439 (1–3) (2013) 148–158.
[42] G.S. Was, J.T. Busby, Role of irradiated microstructure and microchemistry in irradiation-assisted stress corrosion cracking, Phil. Mag. 85 (4–7) (2005) 443–465.
[43] T. Jourdan, F. Soisson, E. Clouet, A. Barbu, Influence of cluster mobility on Cu precipitation in α-Fe: a cluster dynamics modeling, Acta Mater. 58 (9) (2010) 3400–3405.
[44] Z.B. Wang, N.R. Tao, W.P. Tong, J. Lu, K. Lu, Diffusion of chromium in nanocrystalline iron produced by means of surface mechanical attrition treatment, Acta Mater. 51 (14) (2003) 4319–4329.
[45] A.E. Sand, S.L. Dudarev, K. Nordlund, High-energy collision cascades in tungsten: dislocation loops structure and clustering scaling laws, Euro. Phys. Lett. 103 (4) (2013) 46003.
[46] X. Yi, A.E. Sand, D.R. Mason, M.A. Kirk, S.G. Roberts, K. Nordlund, S.L. Dudarev, Direct observation of size scaling and elastic interaction between nano-scale defects in collision cascades, Euro. Phys. Lett. 110 (2015) 36001.
[47] C. Dethloff, E. Gaganidze, J. Aktaa, Quantitative TEM analysis of precipitation and grain boundary segregation in neutron irradiated EUROFER97, J. Nucl. Mater. 454 (1–3) (2014) 323–333.
[48] T.S. Byun, Y. Yang, N.R. Overman, J.T. Busby, Thermal aging phenomena in cast duplex stainless steels, JOM 68 (2) (2016) 507–516.
[49] K.J. Leonard, J.T. Busby, S.J. Zinkle, Aging effects on microstructural and mechanical properties of select refractory metal alloys for space-reactor applications, J. Nucl. Mater. 366 (3) (2007) 336–352.
[50] W. Van Renterghem, M.J. Konstantinović, M. Vankeerberghen, Evolution of the radiation-induced defect structure in 316 type stainless steel after post-irradiation annealing, J. Nucl. Mater. 452 (1–3) (2014) 158–165.

Please cite this article in press as: O.V. Rofman, et al., The natural aging of austenitic stainless steels irradiated with fast neutrons, Journal of Nuclear Materials (2017), https://doi.org/10.1016/j.jnucmat.2017.11.006